

# Loss of Krüppel-like factor 9 facilitates stemness in ovarian cancer ascites-derived multicellular spheroids via Notch1/slug signaling

Kun Wang | Shujie Liu | Zhiyuan Dou | Shuo Zhang | Xingsheng Yang 

Department of Obstetrics and Gynecology, Qilu Hospital of Shandong University, Ji'nan, China

## Correspondence

Xingsheng Yang, Department of Obstetrics and Gynecology, Qilu Hospital of Shandong University, Ji'nan, Shandong, 250012, China. Email: xingshengyang@sdu.edu.cn

## Funding information

National Natural Science Foundation of China (Grant/Award Number: no. 81372809).

## Abstract

The ascites that develops in advanced OC, both at diagnosis and upon recurrence, is a rich source of multicellular spheroids/aggregates (MCSs/MCAs), which are the major seeds of tumor cell dissemination within the abdominal cavity. However, the molecular mechanism by which specific ascites-derived tumor cells survive and metastasize remains largely unknown. In this study, we elucidated cancer stem cell (CSC) properties of ascites-derived MCSs, concomitant with enhanced malignancy, induced EMT, and low KLF9 (Krüppel-like factor 9) expression, compared with PTCs. KLF9 was also downregulated in OC cell line-derived spheroids and the CD117<sup>+</sup>CD44<sup>+</sup> subpopulation in MCSs. Functional experiments demonstrated that KLF9 negatively modulated stem-like properties in OC cells. Mechanistic studies revealed that KLF9 reduced the transcriptional expression of Notch1 by directly binding to the Notch1 promoter, thereby inhibiting the function of slug in a CSL-dependent manner. Clinically, expression of KLF9 was associated with histological grade and loss of KLF9 predicts poor prognosis in OC.

## KEYWORDS

KLF9, multicellular spheroids, Notch1, ovarian cancer stem cells, slug

## 1 | INTRODUCTION

Metastasis of OC is the most common cause of disease-associated mortality. In the majority of cases, the disease has spread beyond ovaries at the time of diagnosis.<sup>1</sup> Metastasis is a dynamic, multi-step and complex process, including escaping from primary tumor, spreading in the systemic circulation, extravasation at distant tissues, and organ seeding.<sup>2</sup> Among diverse metastatic routes, peritoneal

implantation is the most common mode of metastasis for OC.<sup>3</sup> At the cellular level, cancer cells exfoliated from the primary site to a fluid-filled peritoneal cavity where they exist in suspension as single cells or MCSs. OC MCSs contribute to the production and accumulation of large amounts of malignant ascites and are the major seeds of peritoneal metastasis.<sup>4</sup> Therefore, improved understanding of properties, underlying molecular mechanisms of the cellular biology of OC MCSs will shed light on novel therapeutic options.

**Abbreviations:** CCK-8, Cell Counting Kit-8; CHIP, chromatin immunoprecipitation; CSL, CBF1/Su (H)/Lag-1 (also known as RBP-Jkappa); EMT, epithelial mesenchymal transition; EpCAM, epithelial cell adhesion molecule; IRS, immunoreactive score; KD, knocked down; KLF9, Krüppel-like factor 9; MCSs/MCAs, multicellular spheroids/aggregates; MP, main population; N1ICD, Notch1 intracellular domain; OC, ovarian cancer; OCSC, ovarian cancer stem cells; OE, over-expressing; PTCs, primary tumor cells; SFM, serum-free medium; SP, side population; TFs, transcription factors; TSS, transcription start site.

This is an open access article under the terms of the Creative Commons Attribution-NonCommercial-NoDerivs License, which permits use and distribution in any medium, provided the original work is properly cited, the use is non-commercial and no modifications or adaptations are made.

© 2021 The Authors. *Cancer Science* published by John Wiley & Sons Australia, Ltd on behalf of Japanese Cancer Association.

Cancer stem cells share several biological characteristics with normal stem cells, including self-renewal, asymmetric cell division, and resistance to apoptosis induced by an anchorage-independent manner.<sup>5</sup> In addition, a defining phenotype restricted to CSCs is their ability for efficient tumorigenesis, drug resistance, and the acquisition of mesenchymal traits through EMT.<sup>6-8</sup> Based on this property, CSCs are also commonly called tumor-initiating cells which were defined as the ability of a few cells to form a xenograft representative of the parental neoplasm.<sup>5</sup> CSCs frequently express a quiescent state that makes them resistant to chemotherapy and radiotherapy that target actively proliferating cells.<sup>9,10</sup> EMT endows cell plasticity, and enables the generation of CSCs at different steps of the metastatic process.<sup>3</sup> Regarding CSC in OC, OC cells are able to switch between epithelial and mesenchymal states during intraperitoneal implantation. The presence of peritoneal MCSs that can survive and proliferate even in the absence of adhesion to a substrate supports the hypothesis that the disease is driven and sustained by CSC and EMT is involved in the process.

TFs have been documented for the occurrence and development of a variety of cancers.<sup>11</sup> The Krüppel-like factor family of TFs consists of 17 conserved proteins containing zinc finger and modulates diverse biologic processes, including cell differentiation, apoptosis, EMT, and stemness.<sup>12-14</sup> Krüppel-like factor 9 (KLF9) is a TF that binds to GC box elements located in the promoter and has been found to be downregulated in colorectal cancer and endometrial carcinoma.<sup>15-17</sup> In the last few years, KLF9 has been reported to be associated with gastric cancer, breast cancer, hepatocellular carcinoma, and prostate cancer.<sup>18-21</sup> In addition, KLF9 was downregulated in glioblastoma-derived spheroids and inhibited glioblastoma stemness.<sup>22-24</sup> However, the role of KLF9 in ovarian CSCs (OCSCs) remains undefined.

Here we use ascites-derived MCSs and spheres induced from human OC cells to detect the expression and function of KLF9 in tumor-initiating CSCs. We found that KLF9 was differentially expressed between MCSs and PTCs, downregulated during the spheroid-formation process of OC cells. Functional assays showed that KLF9 negatively modulates stem cell-like properties. In the mechanism, KLF9 regulates OCSC via CSL-dependent Notch1/slug signaling, which may inspire new insights on clinical management of OC.

## 2 | MATERIALS AND METHODS

### 2.1 | Patients and tissue samples

Detailed in Appendix S1.

### 2.2 | Cell culture, sphere-forming, and re-differentiation assay

Detailed in Appendix S1.

### 2.3 | Limiting dilution assay

Detailed in Appendix S1.

### 2.4 | RNA extraction and quantitative real-time polymerase chain reaction

Detailed in Appendix S1.

### 2.5 | Western blotting analysis

Detailed in Appendix S1.

### 2.6 | siRNA, plasmid extraction, and lentivirus transfection

Detailed in Appendix S1.

### 2.7 | Cell viability assays

Detailed in Appendix S1.

### 2.8 | Flow cytometry analysis and flow sorting

Detailed in Appendix S1.

### 2.9 | Luciferase activity assay

Detailed in Appendix S1.

### 2.10 | Chromatin immunoprecipitation assay

Detailed in Appendix S1.

### 2.11 | Establishment of subcutaneous xenografts and peritoneal metastasis model in vivo

Detailed in Appendix S1.

### 2.12 | Immunohistochemistry

Detailed in Appendix S1.

## 2.13 | Statistical analysis

Detailed in Appendix S1.

## 3 | RESULTS

### 3.1 | Human OC ascites-derived MCSs exhibit a stem cell-like phenotype

To identify the biological characteristics of ascites-derived MCSs of OC cells, we collected samples of malignant ascites from patients who suffered from peritoneal metastasis after surgery. Flow cytometry and immunofluorescence showed that peritoneal MCSs expressed EpCAM, which is a marker for epithelial malignancies (Figure 1A). Transwell assays showed higher cell migration and invasion capabilities of MCSs cells compared with PTCs (Figure 1B). Flow cytometry illustrated a higher proportion of CD117<sup>+</sup> and CD44<sup>+</sup> cells in MCSs (Figure 1C). Sphere formation assay revealed that denser and larger-sized tumor spheres were formed by peritoneal MCSs cells compared with PTCs (Figure 1D). Limiting dilution assay showed that MCSs cells possessed enhanced self-renewal capacity, as evidenced by stem cell frequencies of  $1/84.6 \pm 14.1$  cells and  $1/269.4 \pm 52.5$  cells for MCSs and PTCs cultures respectively, which were statistically significantly different ( $P = .0272$ ; Figure S1). In addition, qRT-PCR showed a higher level of stemness-related genes, including SOX2, Nanog and Oct-4 in MCSs cells (Figure 1E). To determine the sensitivity to cisplatin, we performed CCK8 assays. As shown in Figure 1F, MCSs cells exhibited stronger drug resistance during treatment than PTCs.

As EMT is involved in metastatic processes, we predicted that OC patient ascites-derived cells would undergo an EMT response when aggregating into MCSs and exhibit a mesenchymal-like phenotype. To confirm this, we measured the level of EMT-TFs (snail, slug, twist, zeb1, and zeb2). Of these TFs, snail, slug and twist were significantly upregulated in MCSs relative to PTCs (Figure 1G). Accordingly, we cultured the PTCs under 3D suspension culture conditions to induce cells into spheroid shapes and observed the change in EMT markers during the process. As the data showed, PTCs were found to undergo an EMT response during sphere formation based on upregulation of vimentin, snail, slug, and twist, and downregulation of E-cadherin (Figure 1H). Furthermore, SB-431542 (a TGF $\beta$ R small molecule inhibitor) treatment resulted in smaller and less cohesive spheroids than the control group by blocking the EMT phenotype as evidenced by a significant decrease in snail, slug and twist mRNA expression (Figure 1I), which indicated that EMT participated in MCSs formation and CSC genesis.

### 3.2 | Downregulated expression of KLF9 in OCSCs

As the KLF family was reported to exert functions in diverse biological processes, including cell differentiation, EMT, and stemness,

we proposed that they might participate in the maintenance of CSC characteristics in OC MCSs. We determined the mRNA level of 9 of the KLFs that were able to generate detectable PCR products in OC tissues and observed that KLF9 was significantly downregulated in MCSs, implying an important role of KLF9 in OCSCs (Figure 2A). This MCSs-specific expression pattern was further observed at mRNA level by qRT-PCR and protein level by western blotting (Figure 2B, C). In addition, we did not find significant changes in the level of KLF9 and ratio of the CD117<sup>+</sup> subgroup in metastatic lesions compared with the primary cancers (Figures S2 and S3). In a previous transcriptome sequencing research (GSE28799),<sup>26</sup> we found downregulated expression of KLF9 in OVCAR-3 spheroids that derived from parental OC cell line OVCAR-3 (Figure 2D). To confirm this, we induced the OC cell lines into spheroids under 3D culture conditions and detected changes in KLF9 expression. As shown in Figure 2E, we found that the mRNA and protein levels of Nanog and SOX2 exhibited an increasing trend when parent cells gradually became denser and larger-sized MCSs. Conversely, the levels of KLF9 decreased, which was consistent with previous reports. Additionally, we observed the increase in KLF9 and decrease in Nanog and SOX2 during re-differentiation of MCSs in complete medium (Figure 2E). In other transcriptome sequencing research (GSE33874),<sup>27</sup> KLF9 was downregulated in SP compared with MP isolated from fresh ascites and obtained from patients with advanced epithelial OC (Figure 2F). Therefore, we isolated CD117<sup>+</sup>CD44<sup>+</sup> and CD117<sup>-</sup>CD44<sup>-</sup> subpopulations from ascites-derived MCSs (Figure 2G) and measured the level of KLF9 in the 2 subsets. As shown in Figure 2H, KLF9 maintained low expression levels in CD117<sup>+</sup>CD44<sup>+</sup> cells.

### 3.3 | Krüppel-like factor 9 negatively modulates stem-like properties in OC cells

As KLF9 was detected to be downregulated in OCSC-enriched populations, we further explored its function in OC cells. First, we detected KLF9 expression in 3 cell lines and conducted spheroid-formation capacity assays (Figure S4). Based on the results, we overexpressed KLF9 in SKOV3 cells and knocked down KLF9 in HO-8910 cells by transfecting the specific plasmid or siRNA. Subsequently, 2 cell lines were cultured in serum-free suspension medium for 7 d to induce spheroids. KLF9 mRNA and protein levels were successfully overexpressed or suppressed by specific plasmid or siRNA (Figure 3A). As expected, KLF9 overexpression inhibited the levels of stemness-like markers such as Nanog and SOX2 (Figure 3A). Flow cytometry analysis revealed that the percent of CD44<sup>+</sup>/CD24<sup>-</sup> cells decreased in KLF9-OE SK-spheres (Figure 3B). Figure 3C showed that spheroids were smaller and less cohesive in the KLF9-OE group. A CCK-8 assay demonstrated that KLF9-OE SK-spheres exhibited lower cell survival during cisplatin treatment than the control group (Figure 3D). Annexin V and PI double staining revealed that cisplatin treatment induced more apoptotic events in KLF9-OE SK-spheres, but considerably fewer apoptotic events

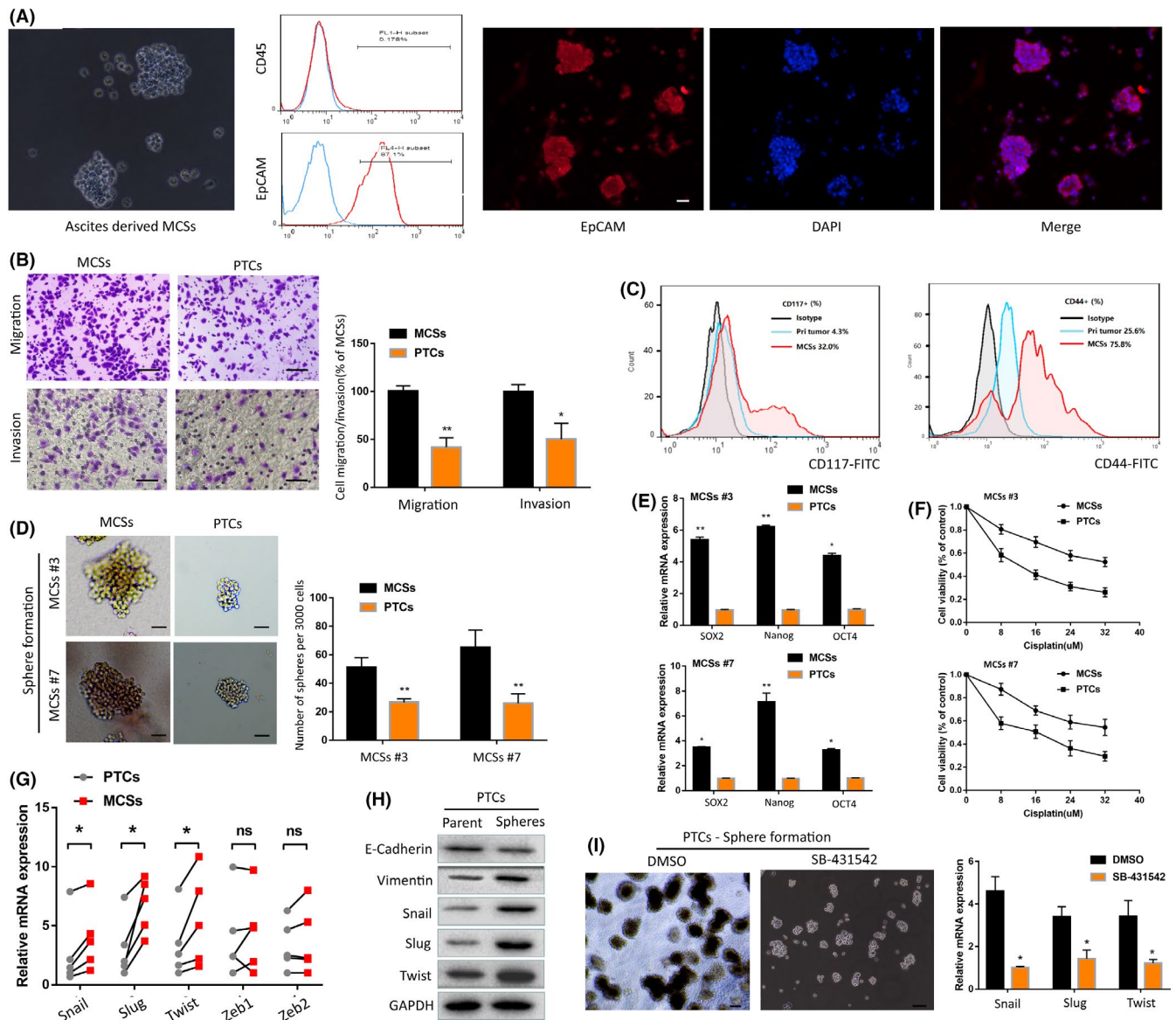


**FIGURE 1** Human OC ascites-derived MCSs exhibit a stem cell-like phenotype. A, Representative image of MCSs isolated from ascites of OC patient (left); CD45 and EpCAM in MCSs were detected by flow cytometry (middle); immunofluorescent staining of EpCAM (red), DAPI (blue) in OC malignant cells from ascites (right) (scale bars, 50 μm). B, Transwell migration and invasion assays of cancer cells derived from primary tumor and MCSs (scale bar, 50 μm). C, Flow cytometry analysis of CD117 and CD44 in cancer cells isolated from primary tumor and MCSs. D, Sphere formation assays of cancer cells derived from primary tumor and MCSs (Patient #3, Patient #7; scale bar, 50 μm). E, qPCR analysis of relative stemness markers, SOX2, Nanog, and Oct4, of cancer cells isolated from primary tumor and MCSs (Patient #3, Patient #7). F, MCSs and primary tumor-derived cells (Patient #3, Patient #7) were treated with cisplatin for 36 h. Cell viability was examined through a CCK-8 assay. G, qPCR analysis of relative EMT-TFs, snail, slug, twist, zeb1, and zeb2, of cancer cells isolated from primary tumor and MCSs of patient samples (n = 5). H, EMT markers of PTCs and PTCs-derived spheroids were detected by western blot. I, Sphere formation assays of PTCs with treatment of DMSO or SB-431542 (scale bar, 50 μm)

in the control group (Figure 3E). Additionally, KLF9-OE SK-spheres exhibited a significantly reduced tumor size and number compared with the control group in a mouse xenograft model (Figure 3F). Immunohistochemical analysis displayed a decrease in CD117 after KLF9 overexpression (Figure 3G), which represented the suppression of the CSC-like phenotype. In contrast, KLF9 knockdown strengthened stemness of HO-8910 cells. As cell proliferation and survival could interfere with the effects of

KLF9 in the spheroid assay, we further investigated cell viability after KLF9 overexpression and knockdown. KLF9 overexpression in SKOV3 and KLF9 knockdown in HO-8910 did not show significant changes in cell viability 5 d after incubation compared with the control by CCK8 (Figure S5), suggesting that the suppressed or strengthened sphere-forming ability would not result from cell survival or proliferation. These results indicated that KLF9 negatively modulates stem-like properties in OC cells.

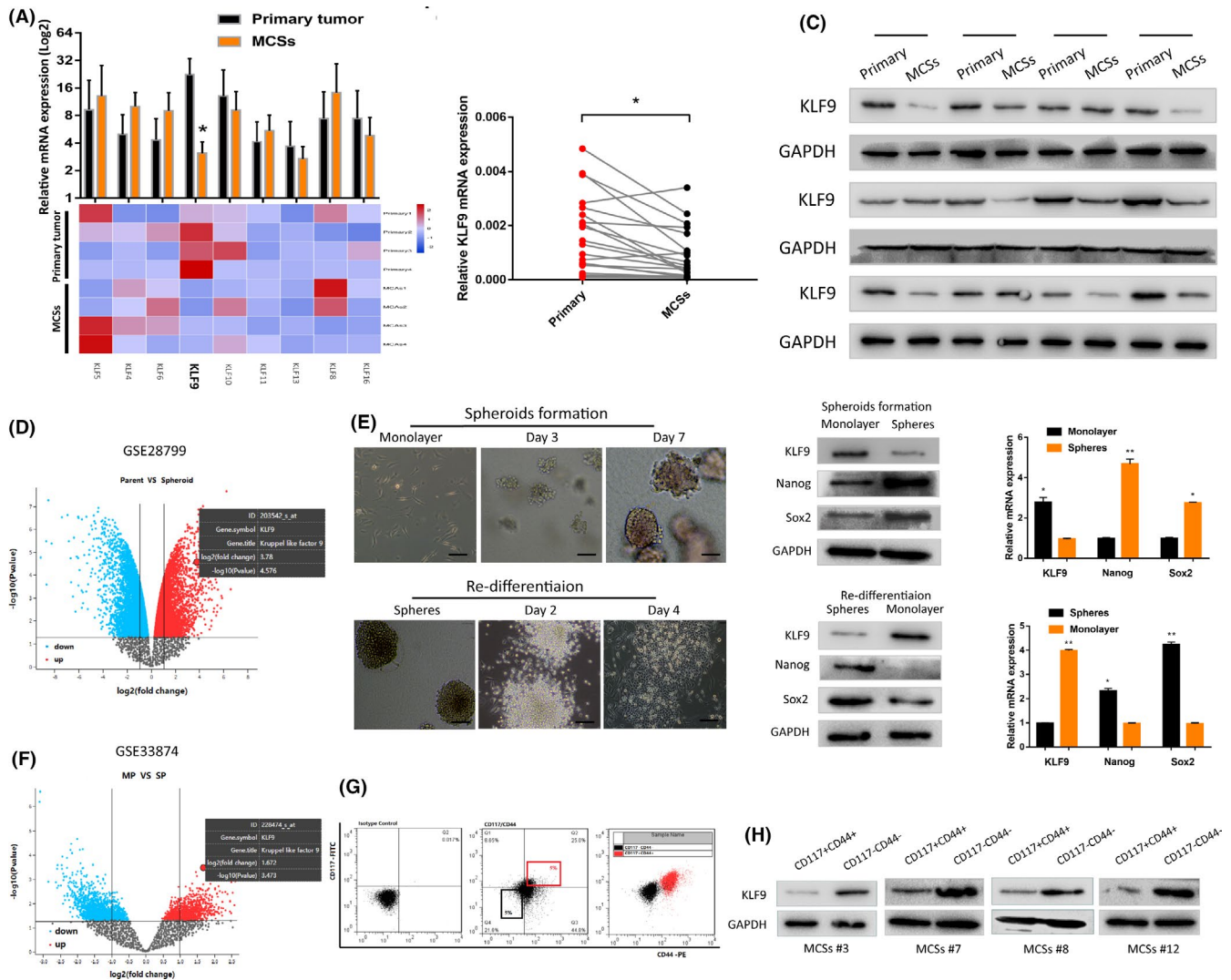


**FIGURE 2** Downregulated expression of KLF9 in OCSCs. A, qRT-PCR was used to detect the expression of 9 of KLFs family in 4 pairs of primary tumor lesions and matched MCSs. B, qRT-PCR was used to detect the expression of KLF9 in 20 pairs of primary tumor lesions and matched MCSs. C, Western blot assay bands of 12 pairs primary tissues and MCSs in ascites of OC patients using ImageJ software. D, Volcano plots depicting differentially expressed genes between parental OC cell line OVCAR-3 and OVCAR-3-induced spheroids (GSE28799). E, Protein and mRNA expression of KLF9, Nanog, and SOX2 of parental SKOV3 cells (monolayer), day 7 spheroid cells derived from SKOV3 cells growing in serum-free medium with growth factors (spheres; upper). Protein and mRNA expression of KLF9, Nanog, and SOX2 of SK-spheroids (spheres) and differentiated cells growing in complete medium (10% serum; Monolayer). F, Volcano plots depicting differentially expressed genes between SP and MP isolated from fresh ascites obtained from patients with advanced epithelial ovarian cancer (GSE33874). G, Isolation of CD117<sup>+</sup>CD44<sup>+</sup> and CD117<sup>-</sup>CD44<sup>-</sup> subsets of ascites-MCSs by FACS. H, Protein level of KLF9 in CD117<sup>+</sup>CD44<sup>+</sup> and CD117<sup>-</sup>CD44<sup>-</sup> subsets of ascites-MCSs detected by western blot

### 3.4 | Slug involves in KLF9-mediated modulation of stem-like phenotype

Considering the critical role of EMT in MCSs formation and acquisition of a stem-like change phenotype, we investigated whether KLF9 regulated the EMT process in OC cells by detecting relative markers. Figure 4A shows that the mRNA and protein levels of the epithelial markers E-cadherin were significantly increased in SKOV3-KLF9 cells. In contrast, the levels of the mesenchymal markers N-cadherin and vimentin were markedly decreased (Figure 4A). As snail, slug and twist among the EMT-TFs were upregulated in MCSs (Figure 1G), we tested the expression of the 3 TFs with KLF9

overexpression in SKOV3 cells. Interestingly, our data showed that with upregulation of KLF9, the mRNA and protein levels of slug significantly decreased. However, the levels of other TFs had no significant changes (Figure 4A). Then, we analyzed the expression of slug in parental, as well as in cancer cell-derived, sphere cells. Western blotting assay showed a higher expression of slug was associated with a lower expression of KLF9 in spheres, compared with those in both SKOV3 and HO-8910 parental cells (Figure 4B). To explore whether slug participated in KLF9-mediated modulation of the stem-like phenotype in OC cells, rescue experiments were performed. As the results showed, the KLF9 overexpression-induced inhibited expression of stemness-related markers (Figure 4C),

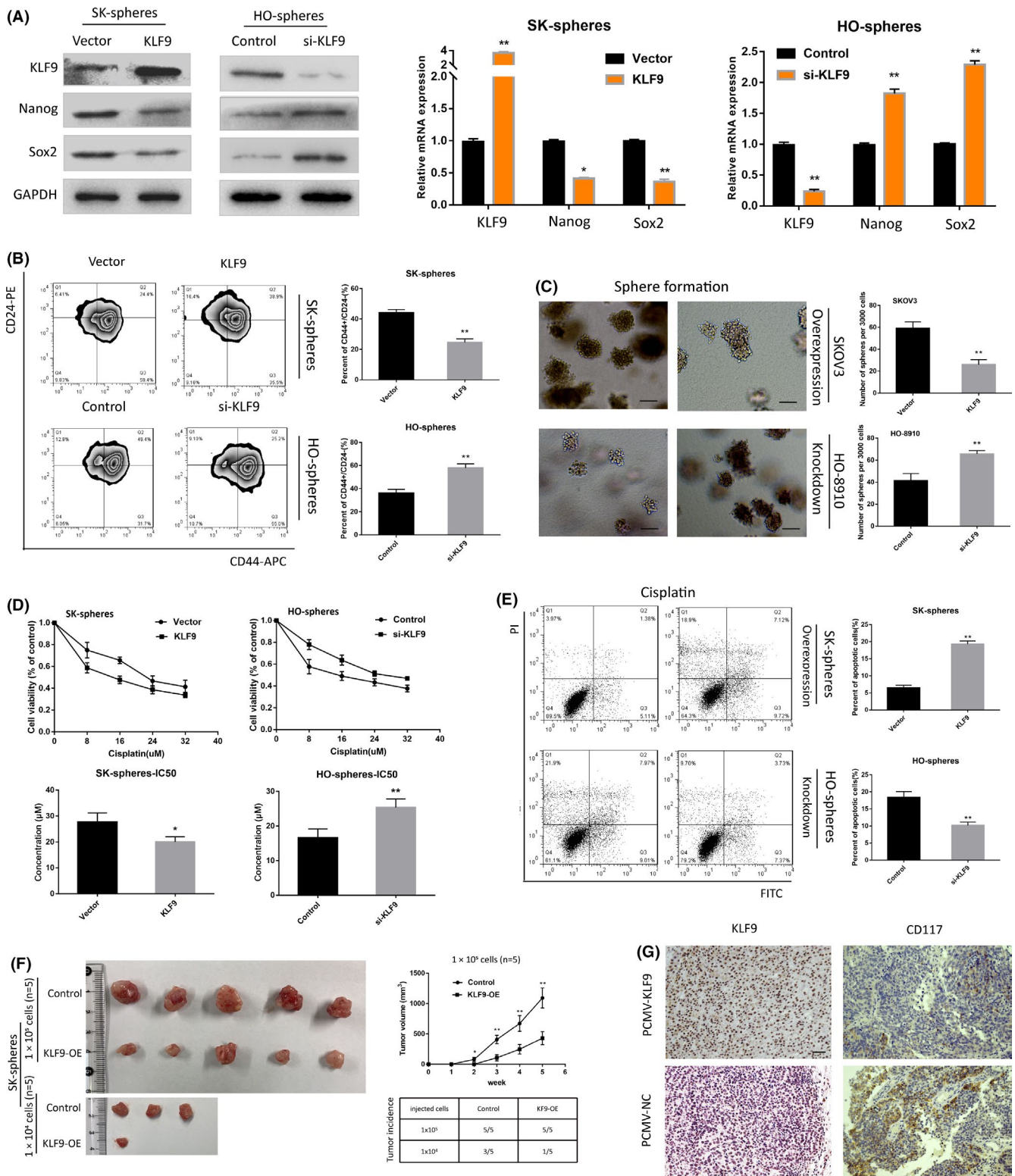


**FIGURE 3** Krüppel-like factor 9 negatively modulates stem-like properties in ovarian cancer cells. A, Expression of KLF9 and stem-related markers, Nanog and SOX2, were detected by western blotting analysis. B, The proportion of CD44<sup>+</sup>CD24<sup>+</sup> in SKOV3 and HO-8910 spheroids was analyzed by FCM and quantitative analysis of flow cytometry. C, Vector, KLF9-OE SKOV3 and NC KLF9-KD HO-8910 cells were cultured in semi-solid serum-free medium for 5 d. The size and number of spheres formed was determined via microscopy and representative pictures are shown. D, Vector, KLF9-OE SKOV3 and NC KLF9-KD HO-8910 cell-derived spheres were treated with cisplatin for 36 h. Cell viability was measured through a CCK-8 assay; the data are presented as the fold change relative to the treatment-free groups. E, Apoptosis cells were evaluated with annexin V and PI staining and analyzed by flow cytometry. F, Effect of KLF9 overexpression on the tumor growth of OC cell-derived spheres *in vivo* was analyzed by inoculating SK-sphere cells into nude mice. G, KLF9 and CD117 immunohistochemical staining were performed in each group of tumors (scale bars, 50 μm)

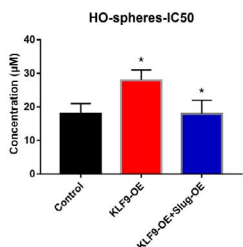
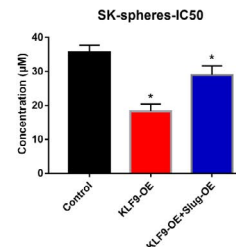
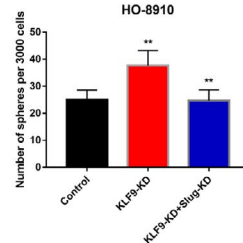
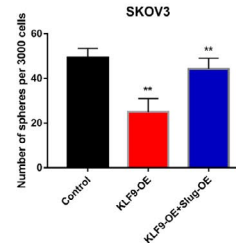
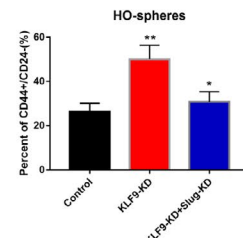
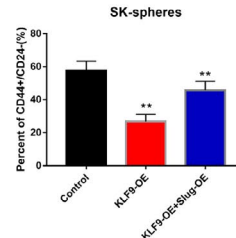
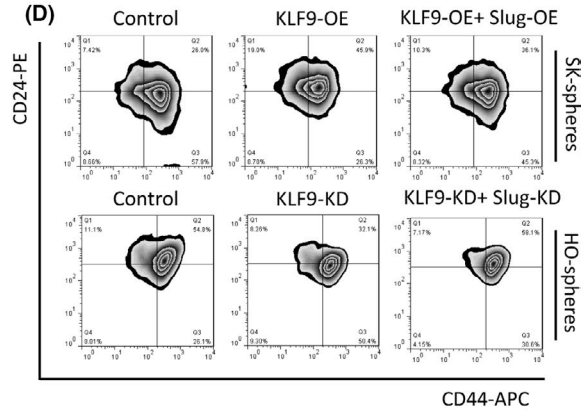
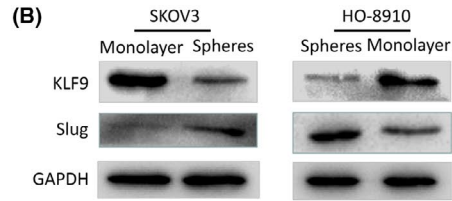
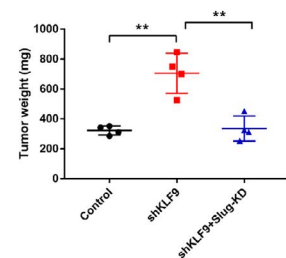
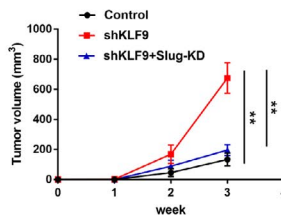
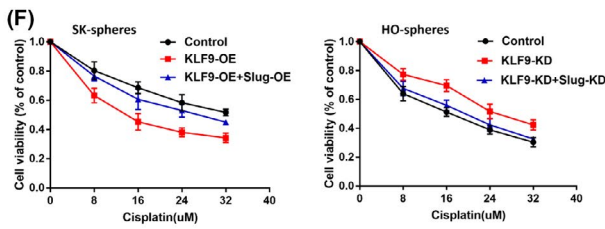
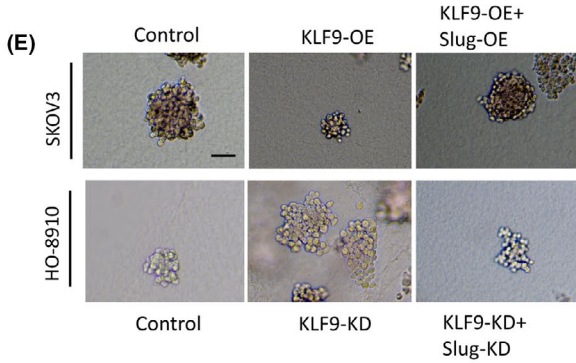
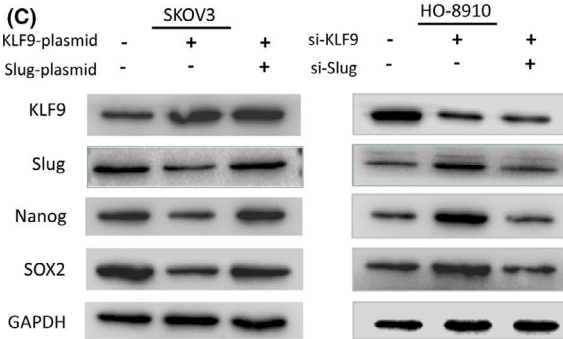
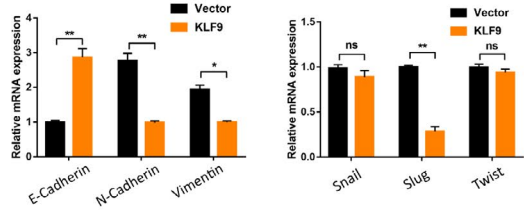
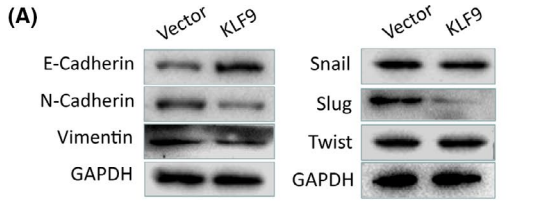


**FIGURE 4** Slug is involved in KLF9-mediated modulation of stem-like phenotype. A, Protein and mRNA expression of EMT markers in control and KLF9-OE SKOV3 cells (left). Protein and mRNA expression of EMT-TFs in control and KLF9-OE SKOV3 cells (right). B, KLF9 and slug expression in monolayer and sphere cells of SKOV3 and HO-8910 were detected by western blotting. C, Stem-markers, Nanog and SOX2, of SKOV3 and HO-8910 spheroids were detected by western blotting. D, Proportion of CD44<sup>+</sup>CD24<sup>-</sup> in SKOV3 and HO-8910 spheroids was analyzed by FCM and quantitative analysis of flow cytometry. E, Sphere formation (sphere >50  $\mu$ m) was assessed (scale bars, 50  $\mu$ m). F, Sensitivity of cells to cisplatin was analyzed by CCK8. G, Effect of sh-KLF9 and sh-KLF9+slug-KD on the growth of HO-spheres in vivo was analyzed

decreased CD44<sup>+</sup>/CD24<sup>-</sup> proportion (Figure 4D), reduced sphere formation capacity (Figure 4E), and increased sensitivity to cisplatin (Figure 4F) were reversed, at least partially, by slug overexpression in SKOV3 cells. In addition, KLF9 knockdown-induced enhanced stemness was reversed by slug knockdown in HO-8910 cells. Finally, an in vivo experiment showed that when sh-slug was introduced into KLF9-KD cells, the tumorigenicity was significantly reduced (Figure 4G).

### 3.5 | Notch1 is the direct downstream target of KLF9 in OC cells

Next, we tried to explore the regulatory mechanisms of KLF9 in slug transcription. Previously, Yang Li et al<sup>18</sup> screened 823 potential KLF9 target genes by analyzing KLF9 ChIP-seq data of 3 cell lines (eGFP-KLF9 overexpression MCF-7 cells, eGFP-KLF9 overexpression HEK293 cells and Flag-KLF9 knockout HepG2 cells) from the human Encyclopedia of DNA Elements (ENCODE) database. We sifted out 15 genes that had been reported to be involved in cancer stemness from the 823 candidates for further verification by qRT-PCR (Figure 5A). The results suggested that Notch1 and CXCR4 could be possible targets of KLF9 (fold change > 2.0). Subsequently, western blotting further demonstrated that Notch1, but not CXCR4, was inhibited by KLF9 (Figure 5B). Then, we performed random examination of clinical specimen sections which confirmed that KLF9 and Notch1 expression correlated negatively (Figure 5C). To verify the regulatory mechanism of KLF9 in Notch1 transcription, we determined that KLF9 could bind to several sequences (Site A, B, C, D; predicted sequence score >10) in the Notch1 promoter region based on the JASPAR database (Figure 5D,E). Then, we constructed wild-type and mutant reporter gene vectors containing KLF9 binding sites in the Notch1 promoter region. Dual-luciferase reporter gene assays showed that ectopic KLF9 expression significantly inhibited Notch1-luciferase activity at site B (ACCCACCCACC) and, after mutation of this site (GAAAAACAAGTTT), the inhibition disappeared (Figure 5E). To verify this direct regulation, ChIP assay and PCR were performed. As shown in Figure 5F, enrichment of the Notch1 promoter fragments was confirmed by PCR using primers flanking the KLF9 binding site (site B). Subsequently, the role of Notch1 in KLF9-mediated stemness was further evaluated with in vitro and in vivo experiments. DAPT is a well known Notch1 signaling inhibitor. Figure 5G,H revealed that DAPT (30  $\mu$ mol/L) significantly

attenuated the KLF9-KD-induced strengthened sphere-forming capacity of HO-8910 cells and increased the CD117<sup>+</sup> proportion. In vivo experiments with mice injected with KLF9-KD HO-sphere cells into the peritoneal cavity also indicated that DAPT reduced tumor dissemination induced by KLF9 knockdown (Figure 5I). These results demonstrated that Notch1 is a direct downstream molecule of KLF9 and is involved in KLF9-mediated suppression of OCSC development.

### 3.6 | Krüppel-like factor 9 regulates the expression of slug via CSL-dependent Notch1 signaling

To determine whether KLF9 modulated slug expression in a Notch1-dependent manner, we performed western blotting assay. As the data showed (Figure 6A), DAPT downregulated the expression of Notch1 and slug. Furthermore, the overexpression of slug after KLF9 knockdown in SKOV3 cells was abolished under DAPT treatment. In addition, a significant negative correlation between the mRNA and protein levels of KLF9 and Notch1, and slug expression was evaluated in ascites-derived MCSs samples (Figure 6B,C). We next investigate whether Notch1 induced slug through a canonical CSL-dependent or CSL-independent pathway. DAPT-induced decrease of slug mRNA expression was abolished when CSL was knocked down using si-RNA (Figure S6; Figure 6D), which indicated that Notch1 regulated slug through CSL. However, the mRNA expression level of slug did not reduce significantly after Hes1 or Hey1 inhibition (Figure S7), suggesting that slug is a target of Notch1/CSL but not the downstream molecule of Hes1 or Hey1. Based on the above results, we speculated that Notch1 directly participated in the transcriptional regulation of slug via CSL. To validate this hypothesis, we constructed a human slug reporter plasmid by subcloning a slug promoter (-2000 to +100 relative to the TSS) into the Wt-pGL3 basic vector and conducted a reporter assay after cotransfection with Notch1 intracellular domain (N1ICD) overexpression plasmid or negative control plasmid. As shown in Figure 6E, N1ICD overexpression significantly increased the Luc activity of the slug promoter compared with the control group. We evaluated the sequence of the slug promoter region and found that there was one putative CSL-binding site (TATGGGAAAA) which was conserved in both human and mouse slug promoters (Figure S8). To investigate the involvement of this putative CSL-binding site in the activation of the slug promoter induced by N1ICD overexpression, we constructed a Mut-pGL3-slug promoter vector by introducing a Mut-CSL-binding site

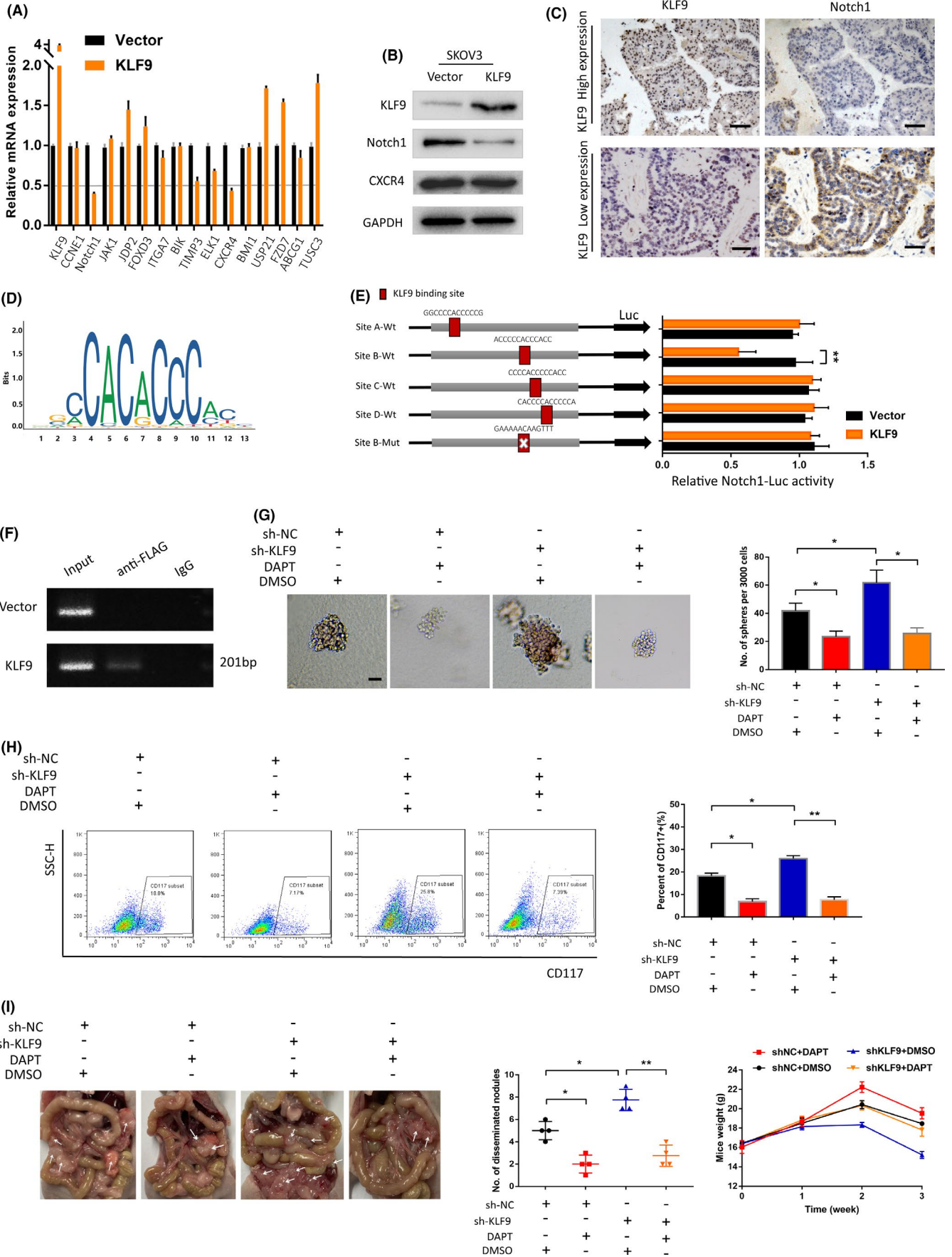


**FIGURE 5** Notch1 is the direct downstream target of KLF9 in OC cells. A, mRNA levels of 15 candidate genes in SKOV3 cells with KLF9 overexpression were detected by qRT-PCR. B, Overexpression of KLF9 substantially downregulated Notch1 expression in SKOV3 cells detected by western blotting. C, Specimen sections from the paraffin-embedded block of OC patients were used for detection with anti-KLF9 and anti-NOTCH1 antibodies, respectively. Scale bar, 50  $\mu$ m. D, Prediction of the sequence logo of KLF9 by the JASPAR database. E, After transfection with vector or KLF9 in HEK293T cells, the relative luciferase activity of mutant or wild-type Notch1 promoter was detected. F, KLF9-binding sites within Notch1 promoter was detected in HO-8910 cells by ChIP assay. G, Representative images of KLF9-KD HO-8910 spheres in the presence or absence of 30  $\mu$ mol/L DAPT for 24 h. Scale bar, 50  $\mu$ m (left). Quantification of spheres (right). H, The proportion of CD117<sup>+</sup> in HO-8910 spheroids was analyzed by FCM and quantitative analysis of flow cytometry. I, Tumor dissemination in peritoneal cavity of KLF9-KD HO-8910 sphere cells and treated with/without DAPT (15 mg/kg)

(TATGGGAAAA→TTTCGCTTAT) and a Del-pGL3-slug promoter vector that lacked the CSL-binding site. Both the mutation and deletion vectors failed to respond to N1ICD overexpression (Figure 6E). These results showed that the CSL-binding site in the slug promoter acts as a Notch1-response element. Furthermore, Figure 6F showed that knockdown of Notch1 or CSL could largely alleviate the transcriptional repression of KLF9 on the promoter of slug conducted by dual-luciferase reporter assay, which provided evidence that KLF9 regulated slug expression in a Notch1-CSL-dependent manner.

### 3.7 | Low expression of KLF9 predicts poor prognosis in OC patients

To assess the prognostic effect of KLF9 in clinical samples, KLF9 expression was examined in 72 paraffin-embedded OC tissues by immunohistochemistry analysis (Figure 7A). The clinicopathological parameters of patients are summarized in Table S2. Results showed that expression of KLF9 was associated with histological grade ( $P = .031$ ; Figure 7B). No statistical significance was found in the correlation between its expression and other parameters including age, histological type, lymphatic metastasis, FIGO stage, residual disease, clinical response, and platinum sensitivity. Kaplan-Meier survival analysis indicated that the patients with low KLF9 expression had a significantly poor prognosis (PFS,  $P = .0447$ ; OS,  $P = .0389$  Figure 7C) compared with those with high KLF9 expression. Furthermore, we used the Kaplan-Meier plotter with TCGA and the GEO databases in which 1656 patients were grouped based on the optimal cutoff value. As shown from the survival curves and cutoff values (Figures 7D, and S9), low KLF9 expression was correlated with poor progression-free survival and overall outcome (PFS,  $P = .0048$ ; OS,  $P = .031$ ).

## 4 | DISCUSSION

Metastasis and chemoresistance, the direct contributor to high recurrence and low survival for the patients, are frequently observed in OC despite decades of effort to optimize therapy options. Here, we aimed to identify critical transcriptional factors that regulate stem cell-like properties of OC and uncover the underlying mechanism. In this study, our data revealed that KLF9 serves as a potent suppressor of OC stemness, by directly binding to the Notch1 promoter and modulating slug expression via the N1ICD/CSL complex. Overall, we uncovered the downregulation of KLF9 in ascites-derived MCSs and

spheres induced from OC cell lines, and disclosed the correlation with tumor differentiation, chemoresistance, and prognosis of OC patients.

Ovarian cancer peritoneal MCSs is a special cell aggregate unit and commonly observed in the malignant ascites of OC patients.<sup>4,28</sup> They are formed by adhesion of c. 10-1000 tumor cells that are exfoliated from the primary tumor site and exhibit suppressed proliferation, but regain the capacity to attach and reinitiate cell division.<sup>28</sup> Studies of breast cancer tissue samples revealed that MCSs in lymphovascular tumor thrombi might have cancer stem cell-like properties.<sup>29</sup> Furthermore, several studies have reported that floating ascites-derived MCSs are a rich source of cells with OCSC traits, including the enhanced capacity of self-renewal, drug resistance, invasion, and high level of stemness-related markers.<sup>30,31-33</sup> Based on these theories, ascites can be viewed as an OCSC-enriched niche, and future research should unravel the molecular mechanisms that are specifically involved in the modulation of OCSC. For example, ascites-derived OC cells exhibit high levels of interleukin-6 (IL-6), STAT3 activation, and enrichment for Wnt ligands, which suggested that the IL-6/JAK/STAT3 axis and Wnt signaling pathway are important effectors of the “communication” between OCSC and the tumor micro-environment.<sup>34-36</sup> In addition, YX Jiang et al.<sup>30</sup> suggested that ascites-derived ALDH<sup>+</sup>CD44<sup>+</sup> tumor cell subsets endowed stemness, metastasis, and metabolic switch via PDK4-mediated signaling in OC.

EMT, regulated by a complex network of genes, is a typical process of embryonic development and tumor progression, and has been proposed as one of the most important biological processes inducing stem cell properties. Initially, the phenomenon was observed in breast cancer. Then many other studies showed it across multiple cancer types.<sup>37</sup> In OC, the classic metastatic journey starts when tumor cells escape from the primary tumor site. Millions of cells are released into the peritoneal cavity and aggregate into EMT-like MCSs, which are slow cycling, invasive, and self-renewing. Conversely, mesenchymal-to-epithelial transition (MET) plays a crucial role in transforming EMT-like MCSs into proliferative epithelial-like tumor cells, leading to metastatic colonization in a distant site.<sup>3</sup> In the present study, we observed induced expression of EMT markers in ascites-derived MCSs. Additionally, the sphere-forming capacity of PTCs was suppressed by treatment with TGF $\beta$  type I receptor inhibitor SB-431542, which implied that EMT participates in MCSs formation and CSC genesis.

In this work, we showed that KLF9 was significantly downregulated in MCSs compared with PTCs. Previous studies have illustrated

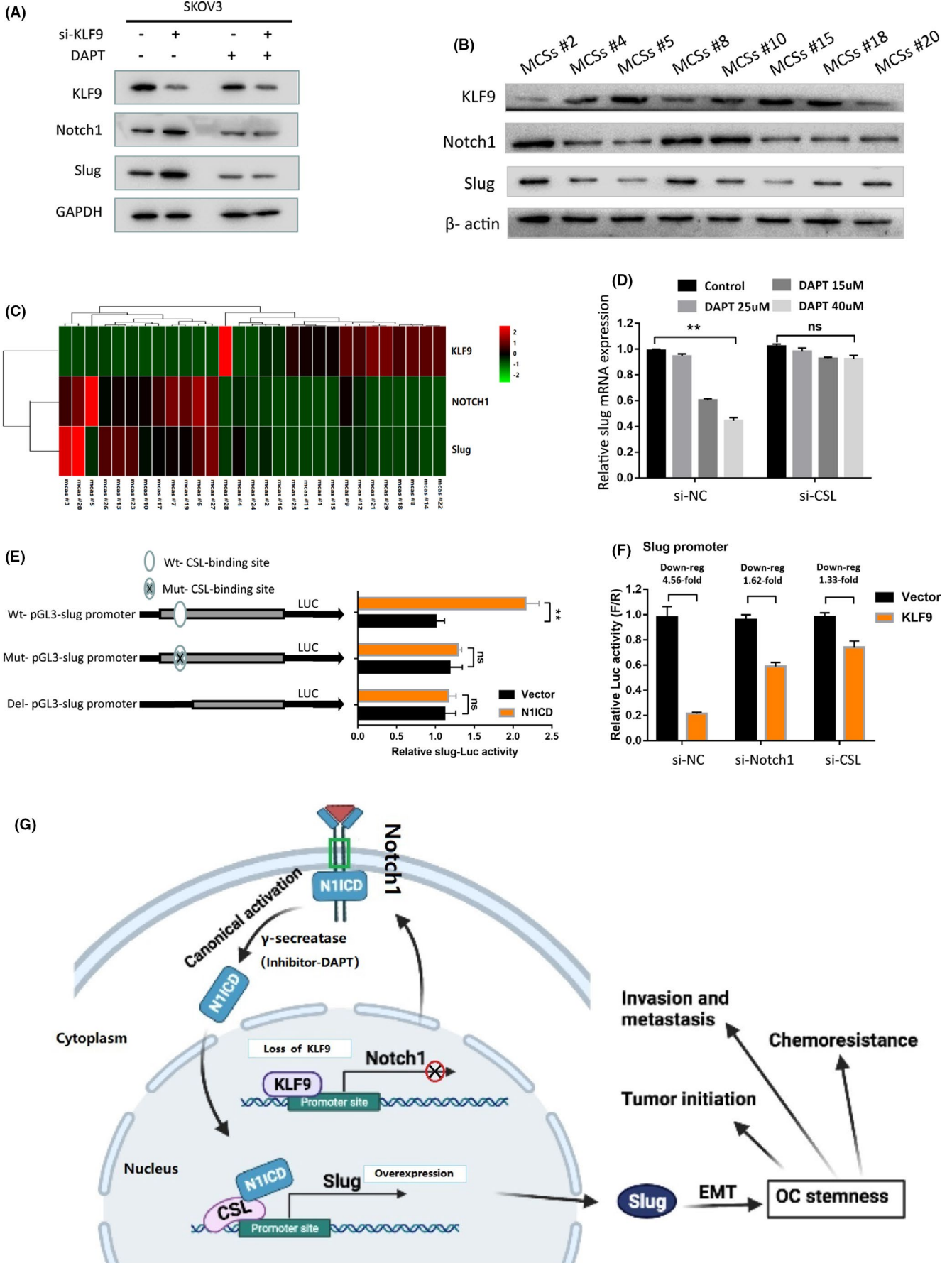
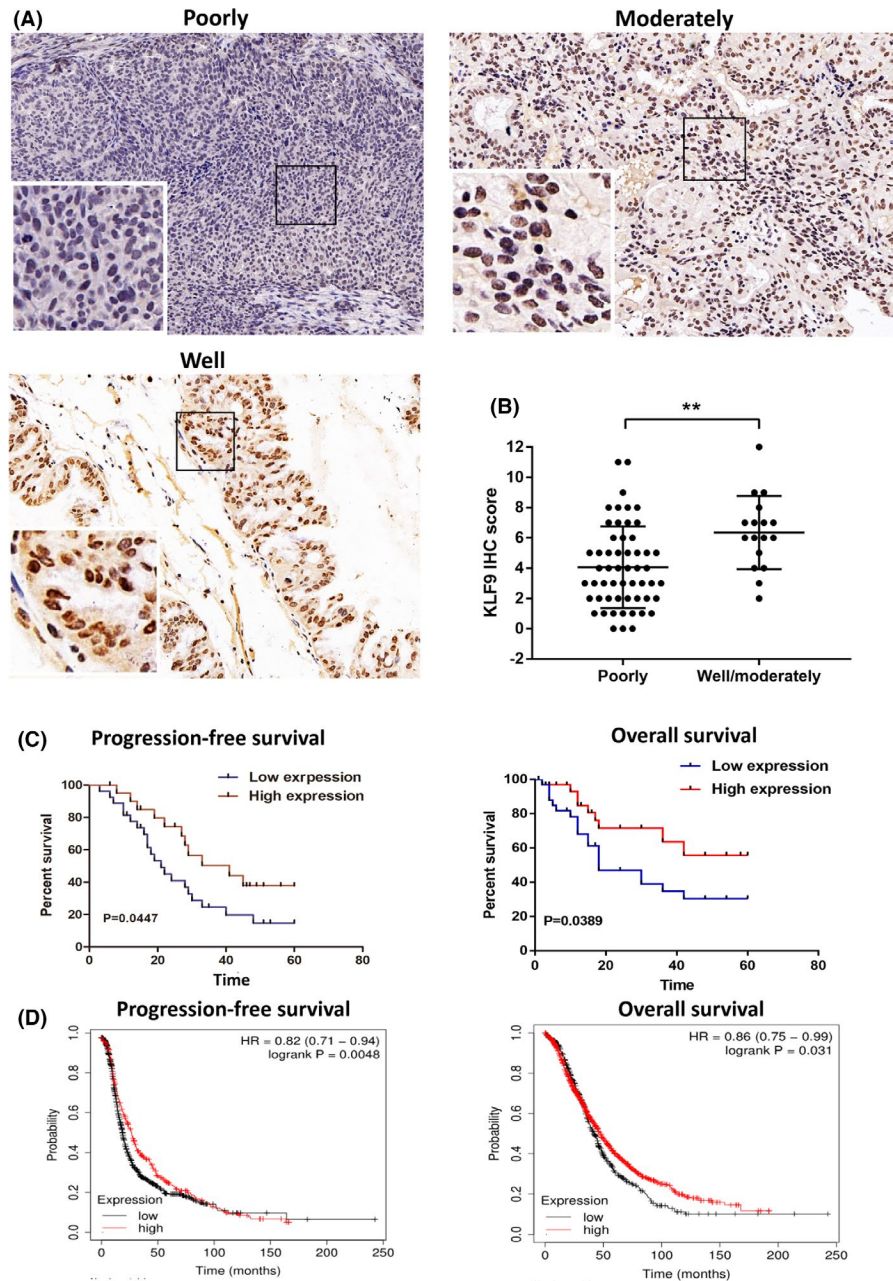


**FIGURE 6** Krüppel-like factor 9 regulates the expression of slug via CSL-dependent Notch1 signaling. A, Expression of KLF9, Notch1 and slug in SKOV3-NC and SKOV3-KLF9-KD cells was detected by western blot after treatment with DAPT or not. B, Expression of KLF9, Notch1, and slug of 8 MCSs samples was detected by western blot. C, Heat-map of KLF9, Notch1, and slug mRNA expression of 29 MCSs samples detected by qRT-PCR. D, Slug mRNA expression was detected by qRT-PCR in SKOV3-NC and SKOV3-CSL-KD cells with treatment of concentration gradients of DAPT. E, After transfection with vector or N1ICD in HEK293T cells, the relative luciferase activity of Wt-CSL, Mut-CSL, or Del-CSL-binding site-slug promoter was detected. F, SKOV3 cells were first transfected with siNotch1, siCSL, or control siRNA. After 36 h, the cells were cotransfected with the pGL3-slug promoter, pRL-TK Renilla luciferase construct and vector, or KLF9 plasmid. Then, relative luciferase activity was detected. G, Schematic summary of the findings of the study. Loss of KLF9 transcriptionally activates Notch1, which directly binds to slug promoter via CSL, ultimately contributing to OC stemness maintenance

**FIGURE 7** Low expression of KLF9 predicts poor prognosis in OC patients. A, Representative IHC staining for KLF9 in well, moderately and poorly differentiated OC tissues. B, IHC score of KLF9 in well/moderately and poorly differentiated OC tissues. C, Progression-free survival (left) and overall survival (right) curves of OC patients were stratified by KLF9 expression. D, The association of KLF9 expression with OC patients' survival from GEO and TCGA database. PFS (left), OS (right)



that KLF9 inhibits glioma cell stemness via diverse signaling pathways and KLF9 induction was found to promote neuroblastoma differentiation by targeting the sonic hedgehog signaling pathway.<sup>22,23,38</sup> But the role of KLF9 in OCSCs and the specific mechanism in OC remains largely unclear. Therefore, we examined the expression

of KLF9 in the process of spheroid formation and re-differentiation of human OC cell lines and found that the expression of KLF9 and stemness-related markers (SOX2, Nanog) showed opposite trends. Furthermore, we overexpressed or knocked down the expression of KLF9 in OC cell lines and found that the CSC phenotype of OC

cells was attenuated or enhanced, suggesting that KLF9 functioned in restraining the stemness of OC cells, which was elaborated for the first time.

For the mechanism, KLF9 overexpression mainly decreased slug expression, compared with other EMT-TFs. Rescue experiments indicated that slug participates in KLF9-mediated modulation of stemness in OC cells. To explore the regulatory mechanism of KLF9 in slug transcription, we utilized the data of ChIP-seq analysis conducted by Yang Li et al.<sup>18</sup> and validated that KLF9 bound directly to the Notch1 promoter. Subsequently, we elaborated that Notch1 directly regulated slug expression in a CSL-dependent pathway. In addition, the repressive role for KLF9 on Notch1/slug expression in OCSC cells was further supported by the potent negative correlation between KLF9 and Notch1/slug mRNA and protein expression in ascites-derived MCSs cases. Although our results indicated that Notch1-CSL/slug was inhibited by KLF9 in OCSC cells, we speculated that there might be other target molecules involved, because of the complexity of transcription factor regulatory networks. Therefore, further research is required to clarify and enrich the KLF9-mediated regulation network in OCSC.

## 5 | CONCLUSIONS

In conclusion, we demonstrated the downregulation of KLF9 in ascites-derived MCSs, spheres induced from OC cell lines, and validated that loss of KLF9 facilitates stem cell-like properties of OCSCs via a CSL-dependent Notch1/slug signaling pathway, which suggested a promising CSCs-specific therapeutic strategy for treatment of OC.

## ACKNOWLEDGMENTS

We thank our colleagues for helpful discussions and valuable assistance. We thank all patients for providing clinical samples and mice sacrificed in this study for their contribution.

## DISCLOSURE

All the authors declare that they have no conflict of interest.

## ORCID

Xingsheng Yang  <https://orcid.org/0000-0002-4946-2033>

## REFERENCES

- Lheureux S, Braunstein M, Oza AM. Epithelial ovarian cancer: evolution of management in the era of precision medicine. *CA: Cancer J Clin.* 2019;69:280-304.
- Lambert AW, Pattabiraman DR, Weinberg RA. Emerging biological principles of metastasis. *Cell.* 2017;168:670-691.
- Celià-Terrassa T, Jolly MK. Cancer stem cells and epithelial-to-mesenchymal transition in cancer metastasis. *Cold Spring Harb Perspect Med.* 2020;10(7):a036905.
- Kristy Shield M, Ackland L, Ahmed N, Rice GE. Multicellular spheroids in ovarian cancer metastases: biology and pathology. *Gynecol Oncol.* 2009;113:143-148.
- Lupia M, Cavallaro U. Ovarian cancer stem cells: still an elusive entity? *Mol Cancer.* 2017;16:64.
- Kim CF, Dirks PB. Cancer and stem cell biology: how tightly intertwined? *Cell Stem Cell.* 2008;3:147-150.
- Battle E, Clevers H. Cancer stem cells revisited. *Nat Med.* 2017;23:1124-1134.
- Kreso A, Dick JE. Evolution of the cancer stem cell model. *Cell Stem Cell.* 2014;14:275-291.
- Chen W, Dong J, Haiech J, Kilhoffer MC, Zeniou M. Cancer stem cell quiescence and plasticity as major challenges in cancer therapy. *Stem Cells Int.* 2016;2016:1740936.
- Takeishi S, Nakayama KI. To wake up cancer stem cells, or to let them sleep, that is the question. *Cancer Sci.* 2016;107:875-881.
- Valastyan S, Weinberg RA. Tumor metastasis: molecular insights and evolving paradigms. *Cell.* 2011;147:275-292.
- McConnell BB, Yang VW. Mammalian Krüppel-like factors in health and diseases. *Physiol Rev.* 2010;90:1337-1381.
- Tetreault MP, Yang Y, Katz JP. Krüppel-like factors in cancer. *Nat Rev Cancer.* 2013;13:701-713.
- Kaczynski J, Cook T, Urrutia R. Sp1- and Kruppel-like transcription factors. *Genome Biol.* 2003;4:206.
- Imataka H, Sogawa K, Yasumoto K, et al. Two regulatory proteins that bind to the basic transcription element (BTE), a GCbox sequence in the promoter region of the rat P-4501A1 gene. *EMBO J.* 1992;11:3663-3671.
- Kang L, Lü B, Jing X, Hu H, Lai M. Downregulation of Kruppel-like factor 9 in human colorectal cancer. *Pathol Int.* 2008;58:334-338.
- Simmen FA, Su Y, Xiao R, Zeng Z, Simmen RC. The Kruppel-like factor 9 (KLF9) network in HEC-1-A endometrial carcinoma cells suggests the carcinogenic potential of dys-regulated KLF9 expression. *Reprod Biol Endocrinol.* 2008;6:41.
- Li Y, Sun Q, Jiang M, et al. KLF9 suppresses gastric cancer cell invasion and metastasis through transcriptional inhibition of MMP28. *FASEB Journal.* 2019;33(7):7915-7928.
- Limame R, de Beeck KO, Van Laere S, et al. Expression profiling of migrated and invaded breast cancer cells predicts early metastatic relapse and reveals Krüppel-like factor 9 as a potential suppressor of invasive growth in breast cancer. *Oncoscience.* 2013;1(1):69-81.
- Sun J, Wang B, Liu Y, et al. Transcription factor KLF9 suppresses the growth of hepatocellular carcinoma cells in vivo and positively regulates p53 expression. *Cancer Lett.* 2014;355:25-33.
- Shen P, Sun J, Xu G, et al. KLF9, a transcription factor induced by influtamide-caused cell apoptosis, inhibits AKT activation and suppresses tumor growth of prostate cancer cells. *Prostate.* 2014;74:946-958.
- Ying M, Tilghman J, Wei Y, et al. Kruppel-like factor-9 (KLF9) inhibits glioblastoma stemness through global transcription repression and integrin alpha6 inhibition. *J Biol Chem.* 2014;289(47):32742-32756.
- Ying M, Sang Y, Li Y, et al. KLF9, a differentiation-associated transcription factor, suppresses Notch1 signaling and inhibits glioblastoma-initiating stem cells. *Stem Cells.* 2011;29(1):20-31.
- Guichet PO, Guelfi S, Teigell M, et al. Notch1 stimulation induces a vascularization switch with pericyte-like cell differentiation of glioblastoma stem cells. *Stem Cells.* 2015;33(1):21-34.
- Correa RJM, Peart T, Valdes YR, DiMattia GE, Shepherd TG. Modulation of AKT activity is associated with reversible dormancy in ascites-derived epithelial ovarian cancer spheroids. *Carcinogenesis.* 2011;33:49-58.
- Wang L, Mezencev R, Bowen NJ, et al. Isolation and characterization of stem-like cells from a human ovarian cancer cell line. *Mol Cell Biochem.* 2012;363(1-2):257-268.
- Vathipadiakal V, Saxena D, Mok SC, et al. Identification of a potential ovarian cancer stem cell gene expression profile from advanced stage papillary serous ovarian cancer. *PLoS One.* 2012;7:e29079.

28. Burlison KM, Boente MP, Pambuccian SE, Skubitz AP. Disaggregation and invasion of ovarian carcinoma ascites spheroids. *J Transl Med.* 2006;4:6.
29. Xiao Y, Ye Y, Yearsley K, Jones S, Barsky S. The lymphovascular embolus of inflammatory breast cancer expresses a stem cell-like phenotype. *Am J Pathol.* 2008;173:561-574.
30. Jiang Y-X, Siu MK-Y, Wang J-J, et al. Ascites-derived ALDH+CD44+ tumour cell subsets endow stemness, metastasis and metabolic switch via PDK4-mediated STAT3/AKT/NF- $\kappa$ B/IL-8 signaling in ovarian cancer. *Br J Cancer.* 2020;123:275-287.
31. Wintzell M, Hjerpe E, Avall Lundqvist E, Shoshan M. Protein markers of cancer-associated fibroblasts and tumor-initiating cells reveal subpopulations in freshly isolated ovarian cancer ascites. *BMC Cancer.* 2012;12:359.
32. Di J, Duiveman-de Boer T, Zusterzeel PL, Figdor CG, Massuger LF, Torensma R. The stem cell markers Oct4A, Nanog and c-Myc are expressed in ascites cells and tumor tissue of ovarian cancer patients. *Cell Oncol.* 2013;36:363-374.
33. Mo L, Bachelder RE, Kennedy M, et al. Syngeneic murine ovarian cancer model reveals that ascites enriches for ovarian cancer stem-like cells expressing membrane GRP78. *Mol Cancer Ther.* 2015;14:747-756.
34. Giuntoli RL 2nd, Webb TJ, Zoso A, et al. Ovarian cancer-associated ascites demonstrates altered immune environment: implications for antitumor immunity. *Anticancer Res.* 2009;29:2875-2884.
35. Saini U, Naidu S, ElNaggar AC, et al. Elevated STAT3 expression in ovarian cancer ascites promotes invasion and metastasis: a potential therapeutic target. *Oncogene.* 2017;36:168-181.
36. Arend RC, Londono-Joshi AI, Samant RS, et al. Inhibition of Wnt/beta-catenin pathway by niclosamide: a therapeutic target for ovarian cancer. *Gynecol Oncol.* 2014;134:112-120.
37. Nieto MA, Huang RYYJ, Jackson RAA, Thiery JPP. EMT: 2016. *Cell.* 2016;166:21-45.
38. Chen S, Song G, Min X, et al. Krüppel-like factor 9 promotes neuroblastoma differentiation via targeting the sonic hedgehog signaling pathway. *Pediatr Blood Cancer.* 2020;67(3):e28108.

#### SUPPORTING INFORMATION

Additional supporting information may be found online in the Supporting Information section.

**How to cite this article:** Wang K, Liu S, Dou Z, Zhang S, Yang X. Loss of Krüppel-like factor 9 facilitates stemness in ovarian cancer ascites-derived multicellular spheroids via Notch1/slug signaling. *Cancer Sci.* 2021;112:4220-4233. <https://doi.org/10.1111/cas.15100>